

# AND NITRIC OXIDE IN AQUEOUS MIXED SOLUTIONS OF SODIUM CHLORITE AND SODIUM HYDROXIDE

EIZO SADA, HIDEHIRO KUMAZAWA, YASUO YAMANAKA,  
ICHIBEI KUDO AND TAKASHI KONDO  
*Department of Chemical Engineering,  
Nagoya University, Nagoya 464*

The rates of single and simultaneous absorptions of dilute  $\text{SO}_2$  and  $\text{NO}$  in aqueous mixed solutions of  $\text{NaClO}_2$  and  $\text{NaOH}$  were measured at  $25^\circ\text{C}$  using a stirred vessel with a plain gas-liquid interface. In the  $\text{SO}_2$ - $\text{NaClO}_2$  system, the absorption rate exceeded the gas-film controlled rate, which implies the possibility of gas-phase oxidation of  $\text{SO}_2$  due to the evolved  $\text{ClO}_2$ . In the  $\text{SO}_2$ - $(\text{NaClO}_2+\text{NaOH})$  system, the absorption rate agreed with that under gas-film controlled conditions. In the  $(\text{SO}_2+\text{NO})$ - $(\text{NaClO}_2+\text{NaOH})$  system, the reduction of the  $\text{NO}$  absorption rate in the presence of  $\text{SO}_2$  substantially exceeded that evaluated through the decrease in interfacial concentration of  $\text{NaClO}_2$  and  $\text{NaOH}$  due to surface reaction with coexisting  $\text{SO}_2$ . The rate of absorption of  $\text{SO}_2$  exceeded the gas-film controlled rate. The decomposition of  $\text{NaClO}_2$  proceeds to a greater degree during simultaneous absorption than the single absorption of  $\text{SO}_2$ .

## Introduction

Nitrogen oxides are one of the major pollutants in the atmosphere and, in addition, have been recognized as essential components in the formation of photochemical smog. Stationary combustion facilities are major sources of these oxides. In this case, more than 90 percent of the nitrogen oxides is inactive nitric oxide with a concentration of several hundred ppm. Thus a considerable amount of research has been directed toward developing a system for the removal of nitric oxide by wet and dry methods. With respect to another air pollutant, sulfur dioxide, several wet scrubbing processes have been developed and their technical systems have been established. The flue gases emitted from fossil-fired facilities generally contain both sulfur and nitrogen oxides. Thus it is convenient to treat sulfur dioxide and nitrogen oxides simultaneously, in the same equipment. In a wet scrubbing process appropriate for the removal of nitrogen oxides there is some possibility of removing sulfur dioxide simultaneously. Otherwise, by some modification of existing wet scrubbing processes for the removal of sulfur dioxide, the nitrogen oxides may also be treated.

Received September 10, 1977. Correspondence concerning this article should be addressed to E. Sada, Dept. of Chem. Eng., Kyoto Univ., Kyoto 606. I. Kudo and T. Kondo are at Dept. of Ind. Eng., Aichi Inst. of Techn., Toyoda 470-03. Y. Yamanaka is now with Tonen Co., Ltd., Kawasaki 210.

In our previous work<sup>7)</sup>, the absorption of nitric oxide by alkaline solutions of sodium chlorite was discussed from the standpoint of chemical absorption to clarify the chemical reaction kinetics. This system is a promising wet scrubbing process for the removal of nitrogen oxides, and further seems to have a possibility of simultaneous treatment of nitrogen oxides and sulfur dioxide. In the present work, single and simultaneous absorptions of dilute nitric oxide and sulfur dioxide were performed in a stirred tank absorber with a plain gas-liquid interface and the kinetics of relevant single and simultaneous absorptions were analyzed on the basis of chemical absorption theory.

## 1. Experimental

Figure 1 shows a schematic diagram of the experimental apparatus. The apparatus is set up in a constant-temperature room. All experimental runs were made using a stirred vessel with a plain gas-liquid interface. The absorber is continuous for the single  $\text{CO}_2$  and  $\text{SO}_2$  absorption runs and batchwise for the single  $\text{NO}$  and simultaneous  $\text{SO}_2$  and  $\text{NO}$  absorption runs. The vessel is sketched in Fig. 2. The vessel, made of acrylic resin, is of 10.0 cm i. d. with four symmetrically located vertical baffles in the liquid phase. The width of each baffle is 1.3 cm. The liquid-phase volume is  $785\text{ cm}^3$  and the gas-phase volume  $573\text{ cm}^3$ .

gas-phase stirrer is a paddle agitator with four flat blades and is placed 3.5 cm above the gas-liquid interface. The liquid-phase stirrer is also a paddle agitator with eight flat blades and is mounted 5.0 cm below the interface. The temperature of the absorber was maintained at 25°C in the water bath.

Solute gases, SO<sub>2</sub> and NO were diluted by N<sub>2</sub>, saturated with water vapor at the temperature of the apparatus and fed into the absorber. The concentrations of SO<sub>2</sub> and NO in the feed stream were varied from 1.1 to 9.6 vol% and 0.5 to 7.5 vol%, respectively. The compositions of SO<sub>2</sub> and NO in the gas streams into and from the absorber were determined by gas chromatography (column: Chromosorb T with 10% dibutylphthalate as a fixed liquid phase at 88°C for SO<sub>2</sub> analysis and molecular sieve 13X at 53°C for NO analysis, carrier gas: N<sub>2</sub>). The concentrations of SO<sub>2</sub> and NO above 0.5 percent could be reproducibly determined by this method. The absorption rates of SO<sub>2</sub> and NO were calculated from the difference between inlet and outlet concentrations and the total gas flow rate.

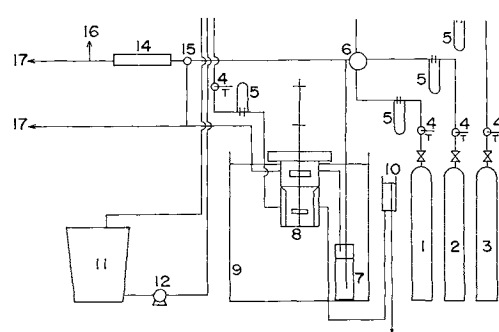
### 1.1 Measurements of liquid-side and gas-side mass transfer coefficients

Prior to the chemical absorption experiments, the physical absorption of pure CO<sub>2</sub> into water was performed at 25°C in the same stirred vessel to determine the liquid-side mass transfer coefficients. The volumetric flow rates of liquid and gas were varied from 2.3 to 9.6 cc/sec and from 1.4 to 3.6 l/min, respectively. Agitator impeller speed in the liquid phase was varied from 40 to 190 rpm, whereas the gas-phase impeller speed was maintained at 400 rpm. The absorption rate was determined by chemical analyses of the inlet and outlet liquids.

In addition, to determine the gas-side mass transfer coefficients, the absorption of lean SO<sub>2</sub> into an aqueous solution of NaOH was carried out with the same absorber. The concentration of SO<sub>2</sub> in the feed stream was approximately 4 percent. The concentration of NaOH in the absorbent was 1.0 mol/l. The absorption process under consideration is believed to be completely gas-film controlled. The impeller speed in the gas phase ranged from 100 to 600 rpm. The volumetric flow rate of gas was varied from 0.97 to 6.31 l/min, whereas the liquid-phase impeller speed was maintained at 100 rpm. The volumetric flow rate of liquid was also kept constant at 3 cc/sec.

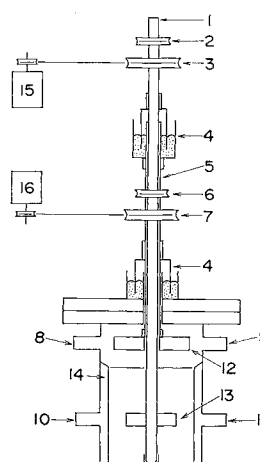
### 1.2 Single and simultaneous absorptions of SO<sub>2</sub> and/or NO in aqueous mixed solutions of NaClO<sub>2</sub> and NaOH

Experiments were performed on the following absorption systems: (1) absorption of SO<sub>2</sub> in aqueous solutions of NaClO<sub>2</sub>, (2) absorption of SO<sub>2</sub>, (3) absorp-



- |                                 |                          |
|---------------------------------|--------------------------|
| 1. N <sub>2</sub> gas cylinder  | 10. Level controller     |
| 2. NO gas cylinder              | 11. Feed tank            |
| 3. SO <sub>2</sub> gas cylinder | 12. Circulating pump     |
| 4. Flow control valve           | 13. Head tank            |
| 5. Orifice flow meter           | 14. Drying column        |
| 6. Gas mixing chamber           | 15. Three-way stop cock  |
| 7. Water vapor saturator        | 16. to gas chromatograph |
| 8. Stirred vessel               | 17. to ventilator        |
| 9. Water bath                   |                          |

Fig. 1 Schematic diagram of experimental apparatus



- |  |
|--|
| 1. Shaft of liquid phase stirrer                 |
| 2. Pulley of tachometer for liquid phase stirrer |
| 3. Pulley for liquid phase stirrer               |
| 4. Mercury seal                                  |
| 5. Shaft of gas phase stirrer                    |
| 6. Pulley of tachometer for gas phase stirrer    |
| 7. Pulley for gas phase stirrer                  |
| 8. Gas inlet                                     |
| 9. Gas outlet                                    |
| 10. Liquid inlet                                 |
| 11. Liquid outlet                                |
| 12. Gas phase stirrer                            |
| 13. Liquid phase stirrer                         |
| 14. Baffle plate                                 |
| 15. Driving motor for liquid phase agitation     |
| 16. Driving motor for gas phase agitation        |

Fig. 2 Detail of stirred tank absorber

tion of NO and (4) simultaneous absorption of SO<sub>2</sub> and NO in aqueous mixed solutions of NaClO<sub>2</sub> and NaOH. The experimental conditions of these systems

	[mol/l]	[mol/l]	[mol/l]	[mol/l]	[mol/l]	[mol/l]	[mol/l]	[mol/l]
SO <sub>2</sub> -NaClO <sub>2</sub>	0.01-0.05	—	0.0041-0.60	—	3.03	3	400	100
SO <sub>2</sub> -NaClO <sub>2</sub> +NaOH	0.01-0.10	—	0.02-1.64	0.01-0.20	3.03	3	400	100
NO-NaClO <sub>2</sub> +NaOH	—	0.01-0.08	0.29-1.64	0.015	1.2	—	400	100
SO <sub>2</sub> +NO-NaClO <sub>2</sub> +NaOH	0.015-0.03	0.007-0.006	0.48-1.64	0.015	1.25	—	400	100

**Table 2** Diffusivity of nitrous oxide in aqueous mixed solutions of sodium chlorite and sodium hydroxide derived from physical absorption data with the liminar liquid-jet at 1 atm and 25°C

Sodium chlorite concentration [mol/l]	Sodium hydroxide concentration [mol/l]	Diffusivity of nitrous oxide [cm <sup>2</sup> /sec]
0.00	0.00	1.66 × 10 <sup>-5</sup>
0.25	0.10	1.62 × 10 <sup>-5</sup>
0.50	0.10	1.60 × 10 <sup>-5</sup>
1.00	0.10	1.57 × 10 <sup>-5</sup>
1.50	0.10	1.52 × 10 <sup>-5</sup>
2.00	0.10	1.46 × 10 <sup>-5</sup>
1.00	0.20	1.58 × 10 <sup>-5</sup>
1.00	0.50	1.23 × 10 <sup>-5</sup>
1.00	0.70	9.48 × 10 <sup>-6</sup>

are given in Table 1.

## 2. Experimental Results and Discussion

### 2.1 Liquid-side and gas-side mass transfer coefficients

The liquid-side mass transfer coefficient,  $k_L^o$ , for absorption of pure CO<sub>2</sub> into water was correlated with the liquid-phase stirring speed  $n_L$  by

$$k_L^o = 6.89 \times 10^{-5} n_L^{0.768} \quad (1)$$

which is valid in the range of 40–190 rpm. The  $k_L^o$  value was independent of liquid flow rate within the experimental conditions.

The gas-side mass transfer coefficient of SO<sub>2</sub>,  $k_G$ , was correlated to the gas-phase stirring speed  $n_G$  in the range of 100–600 rpm by

$$k_G = 6.09 \times 10^{-7} n_G^{0.752} \quad (2)$$

There was negligible effect of the gas flow rate on  $k_G$ . This indicates that the gas phase is completely mixed.

The values of liquid-side and gas-side mass transfer coefficients for gaseous component I were calculated by the following correlations with experimental values of  $k_L^o$  and  $k_G$ , that is,  $k_{L,CO_2-H_2O}^o$  and  $k_{G,SO_2-N_2}$ , respectively.

$$k_{LI}^o = k_{L,CO_2-H_2O}^o (D_I/D_{CO_2-H_2O})^{2/3} \quad (3)$$

$$k_{GI} = k_{G,SO_2-N_2} (\mathcal{D}_I/\mathcal{D}_{SO_2-N_2})^{2/3} \quad (4)$$

### 2.2 Solubility and diffusivity

For the evaluation of the effect of chemical reaction in the liquid phase on the rate of absorption the values of physical solubility and diffusivity of solute gas in the absorbent are required. The interfacial concentrations of NO or SO<sub>2</sub> in aqueous mixed solutions of NaClO<sub>2</sub> and NaOH were calculated from the correla-

tion of gas solubility in mixed electrolyte solutions<sup>5)</sup>:

$$\log(C_{Ji}/C_{Jiw}) = \log(\alpha_J/\alpha_{Jw}) = -(K_B I_B + K_E I_E) \quad (5)$$

$$(J = A_1, A_2)$$

where  $K_B$  and  $K_E$  are the salting-out parameters for the electrolyte B (NaClO<sub>2</sub>) and E (NaOH), respectively. The salting-out parameter depends on the ion and gas present and is expressed by

$$K = x_g + x_a + x_e \quad (6)$$

The values of  $x$  for various species are available in the literature<sup>4,6,7)</sup>:  $x_g(SO_2) = -0.3145$ ,  $x_g(NO) = -0.1825$ ,  $x_a(OH^-) = 0.3875$ ,  $x_a(ClO_2^-) = 0.3497$  and  $x_e(Na^+) = -0.0183$ . The interfacial concentration of SO<sub>2</sub> in water,  $C_{A_1iw}$ , in equilibrium with  $p_{A_1i}$  was evaluated by using Fujita's equation<sup>2)</sup>, whereas the interfacial concentration of NO,  $C_{A_2iw}$ , was estimated by assuming Henry's law ( $H_{A_2} = 1.92 \times 10^{-6}$  mol/cm<sup>3</sup>·atm at 25°C).

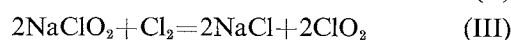
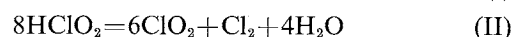
The liquid-phase diffusivity of NO was estimated from the following equation proposed by Joosten and Danckwerts<sup>3)</sup>.

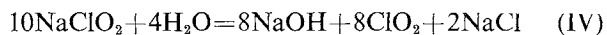
$$(D/D_w)_{NO} = (D/D_w)_{N_2O} \quad (7)$$

Here the value of  $D_w$  for NO in water is available in the literature<sup>10)</sup> ( $2.53 \times 10^{-5}$  cm<sup>2</sup>/sec at 25°C). The diffusivity of N<sub>2</sub>O in the mixed salt solutions was measured in the laminar liquid-jet apparatus. In Table 2, the measured values of N<sub>2</sub>O diffusivity are given as a function of the concentrations of NaClO<sub>2</sub> and NaOH. On the other hand, the reduction of diffusivity of SO<sub>2</sub> in the aqueous solutions was neglected ( $D_{A_1} = 1.90 \times 10^{-5}$  cm<sup>2</sup>/sec at 25°C), because the aqueous solutions were much diluted under the experimental conditions where the diffusion and chemical reaction in liquid phase become significant as compared to the diffusion in gas-film. The effective diffusivities of relevant ions were estimated by the method of Vinograd and McBain<sup>9)</sup>.

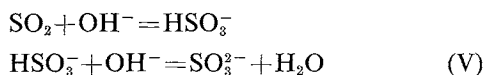
### 2.3 SO<sub>2</sub>-NaClO<sub>2</sub> system

The experimental results for the region  $C_{B0}/C_{A_1i} < 10$  where the effect of gas-film resistance on total mass transfer rate is believed to be less, are shown as a conventional plot of  $\phi_{A_1}$  vs.  $C_{B0}/C_{A_1i}$  in Fig. 3. In an acidic solution, the absorbent NaClO<sub>2</sub> is decomposed by<sup>1)</sup>





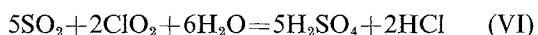
Thus the solute gas  $\text{SO}_2$  reacts mainly with the resulting  $\text{NaOH}$  according to the two-step instantaneous reaction



By considering the stoichiometric relationship between  $\text{NaOH}$  and  $\text{NaClO}_2$  in Reaction (IV), that is  $[\text{NaOH}] = (8/10)[\text{NaClO}_2]$ , the film-theory enhancement factor for the  $\text{SO}_2$ - $\text{NaClO}_2$  system can be approximately given by

$$\phi_{A_1} = 1 + \left( \frac{D_{\text{OH}^-}}{D_{A_1}} \right) \left( \frac{8}{10} \right) \left( \frac{C_{B_0}}{2C_{A_1 i}} \right) \quad (8)$$

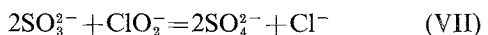
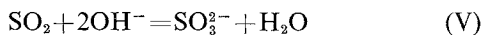
The solid line in Fig. 3 represents the theoretical equation (8) with  $D_{\text{OH}^-}/D_{A_1}$  equal to 1.76. The experimental points deviate considerably from the theoretical line. The deviation exceeds that which might occur in estimating the diffusivity and solubility. It suggests the existence of reaction of  $\text{SO}_2$  with  $\text{ClO}_2$ :



as well as reaction with  $\text{OH}^-$ . In addition, some  $\text{ClO}_2$  desorbs into the gas phase and may oxidize  $\text{SO}_2$ . At present it is difficult to interpret quantitatively the difference between measured and calculated values encountered in Fig. 3. The higher the concentration of  $\text{NaClO}_2$  in the liquid phase, the more  $\text{ClO}_2$  is produced, and correspondingly, it is expected that the amount of  $\text{ClO}_2$  evolved into the gas phase increases. **Figure 4** shows the measurements of  $\text{SO}_2$  absorption rates for a wider range of  $\text{NaClO}_2$  concentration. The chain line in this figure represents the theoretical prediction of absorption rate in a completely gas-film controlled region. The observed absorption rates at  $\text{NaClO}_2$  concentrations greater than 0.2 molar significantly exceed the absorption rate under completely gas-film controlled conditions. This implies the possibility of occurrence of gas-phase oxidation of  $\text{SO}_2$  by the evolved  $\text{ClO}_2$  and supports the existence of Reaction (VI) in the liquid phase.

#### 2.4 $\text{SO}_2$ - $(\text{NaClO}_2 + \text{NaOH})$ system

The reaction prevailing for the present system proceeds under an alkaline situation and hence the decomposition of  $\text{NaClO}_2$  according to Reaction (IV) is suppressed. Thus it is considered that the dissolved  $\text{SO}_2$  reacts with  $\text{OH}^-$  to form  $\text{SO}_3^{2-}$  and  $\text{SO}_3^{2-}$  is oxidized by  $\text{ClO}_2^-$  to form  $\text{SO}_4^{2-}$ :



It follows from the above reaction scheme that the rate of  $\text{SO}_2$  absorption is independent of  $\text{NaClO}_2$  concentration if  $\text{OH}^-$  comes only from the  $\text{NaOH}$  added.

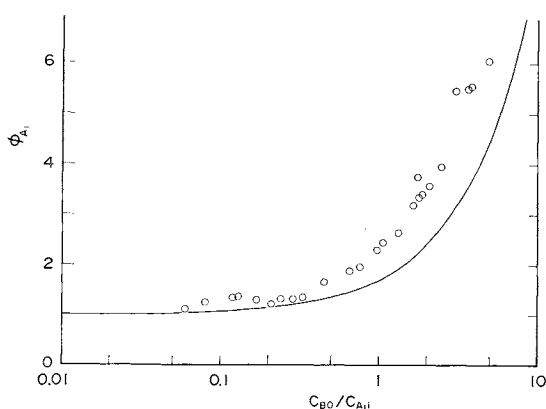


Fig. 3 Plots of  $\phi_{A_1}$  vs.  $C_{B_0}/C_{A_1 i}$  for  $\text{SO}_2$  absorption into an aqueous solution of  $\text{NaClO}_2$

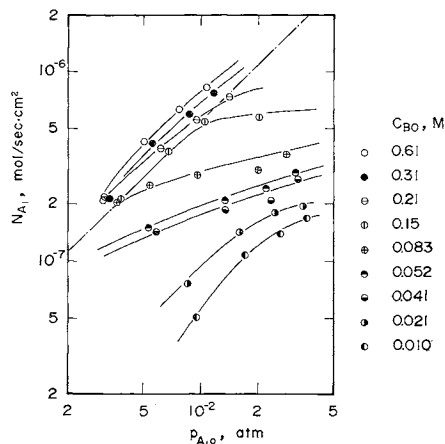


Fig. 4 Effect of  $\text{NaClO}_2$  concentration on  $\text{SO}_2$  absorption rate ( $\text{SO}_2$ - $\text{NaClO}_2$  system)

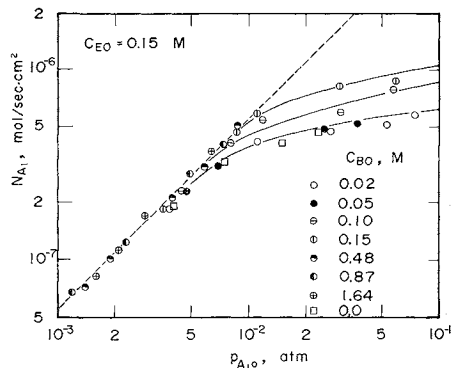


Fig. 5 Effect of  $\text{SO}_2$  concentration on absorption rate ( $\text{SO}_2$ - $(\text{NaClO}_2 + \text{NaOH})$  system)

But **Fig. 5** shows that the presence of  $\text{NaClO}_2$  affects the absorption rate for  $C_{B_0} < 0.15$  molar. In the range of  $C_{B_0} < 0.15$  molar and  $0.0012 < p_{A_1 o} < 0.011$  atm, the absorption rate agrees with that under completely gas-film controlled conditions. There is no promotion in absorption rate as observed in the  $\text{SO}_2$ - $\text{NaClO}_2$  system. From this experimental evidence,

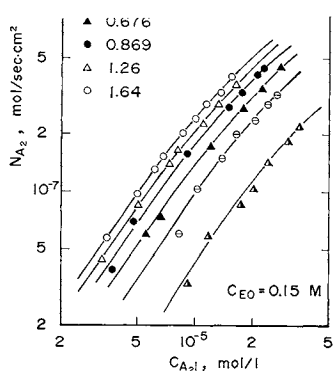


Fig. 6 Relationship between  $N_{A_2}$  and  $C_{A_2i}$  as a parameter of  $\text{NaClO}_2$  concentration ( $\text{NO}-(\text{NaClO}_2 + \text{NaOH})$  system)

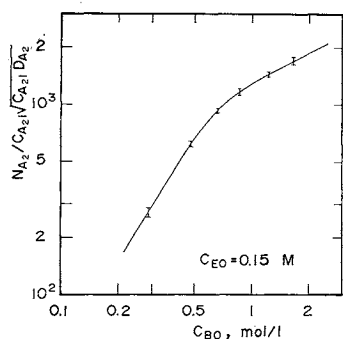
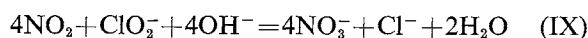
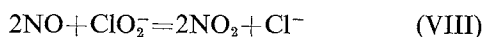


Fig. 7 Effect of  $\text{NaClO}_2$  concentration on  $N_{A_2}/C_{A_2i} \sqrt{C_{A_2i} D_{A_2}}$

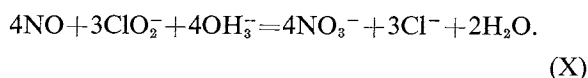
some  $\text{NaClO}_2$  decomposes to form  $\text{OH}^-$  and  $\text{ClO}_2^-$  even in the presence of  $\text{NaOH}$ , but the amount of  $\text{ClO}_2^-$  produced is not large enough to desorb into the gas phase and oxidize  $\text{SO}_2$ .

### 2.5 $\text{NO}-(\text{NaClO}_2 + \text{NaOH})$ system

The reaction between  $\text{NO}$  and  $\text{ClO}_2^-$  in an alkaline solution is considered to be<sup>7)</sup>



The overall reaction reduces to



Here it is assumed that the chemical reaction is regarded as the  $m$ -th order for  $\text{NO}$  and the  $n$ -th order for  $\text{ClO}_2^-$ . Then the order of reaction relative to  $\text{NO}$  can be derived from the slope  $(m+1)/2$  of a logarithmic plot of  $N_{A_2}$  vs.  $C_{A_2i}$ , when the chemical absorption process lies in a fast-reaction regime and the rate of  $\text{NO}$  absorption can be given by

$$N_{A_2} = \sqrt{\frac{2}{m+1}} k C_{B0}^n C_{A_2i}^{m+1} D_{A_2} \quad (9)$$

The validity of this assumption was confirmed in the

of 1.5 for lower values of  $C_{A_2i}$ . According to Eq. (9), a slope of 1.5 means that the order of reaction in  $\text{NO}$  is equal to 2.

Figure 7 shows the effect of  $\text{NaClO}_2$  concentration on absorption rate. The ordinate in the same figure is related to

$$N_{A_2}/C_{A_2i} \sqrt{C_{A_2i} D_{A_2}} = \sqrt{(2/3)} k C_{B0}^n \quad (10)$$

which is derived by substituting 2 into  $m$  in Eq. (9) and rearranging the resulting equation. For low concentrations of  $\text{NaClO}_2$ , dependence of  $N_{A_2}$  on  $C_{B0}$  was very high and no simple relationship between the two factors could be derived. Only for  $C_{B0}$  greater than ca. 0.8 molar did a linear relationship with the slope of 0.5 appear. The order of reaction in  $\text{NaClO}_2$  can be determined as unity. Thus, for  $C_{B0} > 0.8$  molar and the partial pressures covering the present experiment ( $0.003 > p_{A_2o} > 0.018$  atm), the rate constant of the third-order reaction is determined to be  $2.1 \times 10^{12}$  ( $l/\text{mol})^2/\text{sec}$ . In the previous paper<sup>7)</sup> the effect of  $\text{NaOH}$  concentration on the rate constant was empirically correlated by

$$k = 3.80 \times 10^{12} \exp(-3.73 C_{E0}) \quad (11)$$

in the range of  $0.05 < C_{E0} < 0.5$  molar.

The rate constant estimated from Eq. (11) with  $[\text{NaOH}] = 0.15$  molar is  $2.17 \times 10^{12}$  ( $l/\text{mol})^2/\text{sec}$  and coincides well with the experimentally derived value.

### 2.6 $(\text{NO} + \text{SO}_2) - (\text{NaClO}_2 + \text{NaOH})$ system

1) Effect of the presence of  $\text{SO}_2$  on the  $\text{NO}$  absorption rate The rate-controlling step for the absorption of  $\text{SO}_2$  is the diffusion process in the gas film because of high concentration of  $\text{NaClO}_2$ . At a gas-liquid interface,  $\text{SO}_2$  reacts with  $\text{OH}^-$  and  $\text{ClO}_2^-$  through Reactions (V) and (VII). Therefore, it is expected that the interfacial concentrations of  $\text{NaClO}_2$  and  $\text{NaOH}$  in the liquid phase,  $C_{Bi}$  and  $C_{Ei}$ , become low as compared to the bulk concentrations,  $C_{B0}$  and  $C_{E0}$ . The reduction of  $\text{NaClO}_2$  concentration results in a decrease of  $\text{NO}$  absorption rate, while the reduction of  $\text{NaOH}$  concentration results in an increase of  $\text{NO}$  absorption rate.

Figure 8 shows the relations of  $N_{A_2}$  vs.  $C_{A_2i}$  as a parameter of the feed composition of  $\text{SO}_2$ . The reduction of the  $\text{NO}$  absorption rate in the presence of  $\text{SO}_2$  increases with feed composition of  $\text{SO}_2$ . On the other hand, the reduction decreases with increase in  $\text{NaClO}_2$  concentration. Some quantitative interpretation for the reduction in absorption rate is made by a procedure similar to that of Teramoto *et al.*<sup>8)</sup>

From above consideration, the absorption of  $\text{NO}$  into an aqueous mixed solution of  $\text{NaClO}_2$  and  $\text{NaOH}$  with concentrations  $C_{B0}$  and  $C_{E0}$ , respectively, in the

$C_{Ei}(C_{Bi} < C_{B0}$  and  $C_{Ei} < C_{E0}$ ) in the absence of  $SO_2$ . The interfacial concentrations of  $NaClO_2$  and  $NaOH$  during the simultaneous absorption of  $NO$  and  $SO_2$  can be estimated from the material balances at the interface:

$$N_{A_1} = k_{G A_1}(p_{A_1} - 0) = 2k_{L, ClO_2^-}(C_{B0} - C_{Bi}) \\ = (1/2)k_{L, OH^-}(C_{E0} - C_{Ei}) \quad (12)$$

The coefficients 2 and 1/2 in the right-hand sides of Eq. (12) are derived from reciprocals of stoichiometric factors based on the reaction equations (V) and (VII).  $k_{L, ClO_2^-}$  and  $k_{L, OH^-}$  are liquid-side mass transfer coefficients of  $ClO_2^-$  and  $OH^-$  and are estimated to be  $2.18 \times 10^{-3}$  cm/sec and  $4.23 \times 10^{-3}$  cm/sec, respectively ( $D_{ClO_2^-} = 1.72 \times 10^{-5}$  cm<sup>2</sup>/sec and  $D_{OH^-} = 3.34 \times 10^{-5}$  cm<sup>2</sup>/sec). Once estimating  $C_{Bi}$  and  $C_{Ei}$  from Eq. (12), the absorption rate of  $NO$  can be derived by the aid of Fig. 7 and Eq. (11). Figure 9 compares the absorption rates of  $NO$  thus estimated,  $N_{A_2, cal}$ , with those measured during simultaneous absorption of  $NO$  and  $SO_2$ ,  $N_{A_2, obs}$ . As a whole,  $N_{A_2, cal}$  is considerably larger than  $N_{A_2, obs}$ . The calculated interfacial concentration of  $ClO_2^-$  exceeds approximately 95 percent of its bulk concentration, whereas the  $OH^-$  concentration at the interface amounts to 49 percent of its bulk concentration for feed composition of  $SO_2$  equal to 1.5 percent. For  $p_{A_1} = 0.03$  atm, the  $OH^-$  is completely depleted at the interface. Thus, the decomposition of  $NaClO_2$  near the interface is promoted and the chlorite concentration is further decreased. The fact that the concentration of  $OH^-$  near the interface becomes low enough to decompose  $NaClO_2$  is also supported by the following experimental evidence.

2) Effect of the presence of  $NO$  on the  $SO_2$  absorption rate As shown in Fig. 5, the process of  $SO_2$  absorption in the absence of  $NO$  is completely gas-film controlled. However, the absorption rate of  $SO_2$  in the presence of  $NO$  exceeded the completely gas-film controlled rate of absorption. Figure 10 shows experimental results for simultaneous absorption. The abscissa is absorption rate of  $NO$  and the ordinate is that of  $SO_2$ . These experimental results suggest the possibility of occurrence of gas-phase reaction, as stated in a previous section. More of the  $OH^-$  is consumed during the simultaneous absorption of  $SO_2$  and  $NO$  than during the single absorption of  $SO_2$ . Some of the decomposition product  $ClO_2$  diffuses back into the gas phase and oxidizes  $SO_2$ .

## Conclusion

In the system  $SO_2$ - $NaClO_2$ , the absorption rate of  $SO_2$  exceeds the gas-film controlled rate, which implies

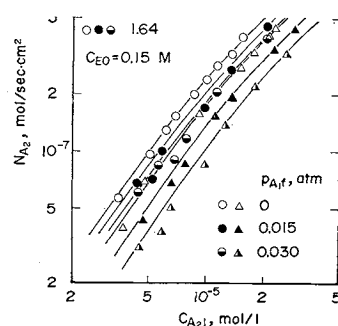
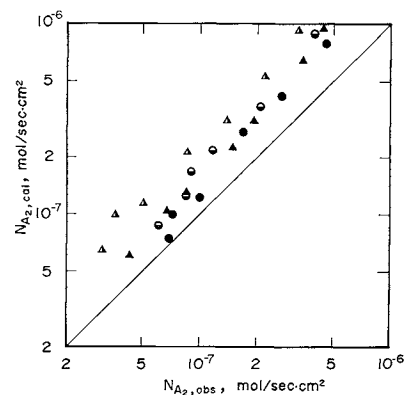


Fig. 8 Effect of  $SO_2$  concentration on  $NO$  absorption rate ( $NO+SO_2$ )-( $NaClO_2+NaOH$ ) system)



Keys as in Fig 8

Fig. 9 Comparison of experimental results with theoretical predictions for  $NO$  absorption rates ( $NO+SO_2$ )-( $NaClO_2+NaOH$ ) system)

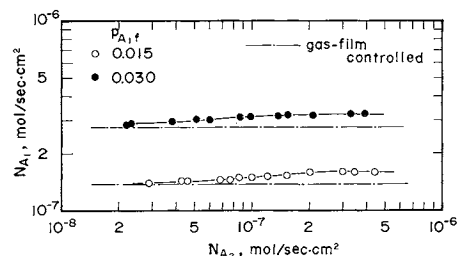


Fig. 10 Effect of  $NO$  absorption rate on  $SO_2$  absorption rate

the possibility of the presence of gas-phase oxidation of  $SO_2$  due to the evolved  $ClO_2$ .

In the  $SO_2$ -( $NaClO_2+NaOH$ ) system, the absorption rate agrees with that under gas-film controlled conditions. In the ( $SO_2+NO$ )-( $NaClO_2+NaOH$ ) system, the reduction of the  $NO$  absorption rate in the presence of  $SO_2$  considerably increased over that derived through the decrease in interfacial concentrations of  $NaClO_2$  and  $NaOH$  due to surface reaction with  $SO_2$ , and the rate of  $SO_2$  absorption exceeded the gas-film controlled rate. Judging from this

## Acknowledgment

The authors wish to express their thanks to Takeda Science Foundation for its financial support.

## Nomenclature

$C$	= concentration in liquid phase	[mol/l]
$D$	= diffusivity in liquid phase	[cm <sup>2</sup> /sec]
$\mathcal{D}$	= diffusivity in gas phase	[cm <sup>2</sup> /sec]
$H$	= Henry's law constant	[mol/cm <sup>3</sup> ·atm]
$I$	= ionic strength	[g-ion/l]
$K$	= salting-out parameter	[l/mol]
$k$	= rate constant of ( $m, n$ )-th order reaction	[(l/mol) <sup><math>m+n-1</math></sup> /sec]
$k_G$	= gas-side mass transfer coefficient	[mol/sec·cm <sup>2</sup> ·atm]
$k_L$	= liquid-side mass transfer coefficient	[cm/sec]
$m$	= order of reaction relative to absorbing component	
$N$	= absorption rate	[mol/sec·cm <sup>2</sup> ]
$n$	= order of reaction relative to liquid-phase reactant	
$n_G$	= agitation speed in gas phase	[rpm]
$n_L$	= agitation speed in liquid phase	[rpm]
$p$	= partial pressure	[atm]
$V_G$	= volumetric gas flow rate	[l/min]
$V_L$	= volumetric liquid flow rate	[cc/sec]
$x_a, x_c, x_g$	= contribution to $K$ of anions, cations and the gas, respectively	[l/g-ion]
$\alpha$	= Bunsen absorption coefficient	[cm <sup>3</sup> of gas/cm <sup>3</sup> of solution]
$\phi$	= enhancement factor	

$B$	= liquid-phase reactant B (NaClO <sub>2</sub> )
$E$	= liquid-phase reactant E (NaOH)
$f$	= feed stream
$i$	= gas-liquid interface
$o$	= outlet
$w$	= water
$0$	= initial value
<Superscript>	
°	= without reaction

## Literature Cited

- 1) Amatsu, H.: *J. Japanese Tech. Assoc. of Pulp and Paper Industry*, **10**, 416 (1956).
- 2) Fujita, S.: *Kagaku Kōgaku*, **27**, 112 (1963).
- 3) Joosten, G. E. H. and P. V. Danckwerts: *J. Chem. Eng. Data*, **17**, 452 (1972).
- 4) Onda, K., E. Sada, T. Kobayashi, S. Kito and K. Ito: *J. Chem. Eng. Japan*, **3**, 18 (1970).
- 5) Onda, K., E. Sada, T. Kobayashi, S. Kito and K. Ito: *ibid.*, **3**, 137 (1970).
- 6) Sada, E., H. Kumazawa, N. Hayakawa, I. Kudo and T. Kondo: *Chem. Eng. Sci.*, **32**, 1171 (1977).
- 7) Sada, E., H. Kumazawa, I. Kudo and T. Kondo: *ibid.*, **33**, 315 (1978).
- 8) Teramoto, M., T. Kitagawa and H. Teranishi: *Kagaku Kogaku Ronbunshu*, **3**, 99 (1977).
- 9) Vinograd, J. R. and J. W. McBain: *J. Am. Chem. Soc.*, **63**, 2008 (1941).
- 10) Wise, D. L. and G. Houghton: *Chem. Eng. Sci.*, **23**, 1211 (1968).

(Presented at the 11th Autumn Meeting of The Soc. of Chem. Engrs., Japan, at Tokyo, October 1977.)